Ultrafast Laser Excitation of CO/Pt(111) Probed by Sum Frequency Generation: Coverage Dependent Desorption Efficiency

Frédéric Fournier, Wanquan Zheng, Serge Carrez, Henri Dubost, and Bernard Bourguignon*

Laboratoire de Photophysique Moléculaire, CNRS, Bâtiment 210, Université de Paris-Sud, 91405 Orsay Cedex, France

(Received 4 August 2002; revised manuscript received 29 January 2004; published 27 May 2004)

CO photodesorption from Pt(111) induced by femtosecond laser pulses is probed by IR + visible sum frequency generation (SFG). Steady state analysis of SFG spectra at varying CO pressure and laser fluence allows one to measure a ≈ 5 orders of magnitude decrease of the photodesorption rate constant when CO coverage decreases from 0.37 to 0.07 monolayer. We ascribe this effect in the framework of the Menzel-Gomer-Redhead mechanism to electron delocalization in the CO layer. The lifetime of electronic excitation decreases when coverage decreases.

DOI: 10.1103/PhysRevLett.92.216102 PACS numbers: 82.53.St, 78.47.+p, 79.20.La

Laser induced photodesorption is an important basic phenomenon related to surface chemistry and its control by electrons. Several aspects of photodesorption are at least semiquantitatively understood in the framework of the Menzel-Gomer-Redhead (MGR) mechanism [1], desorption induced by multiple electronic excitations, and electronic friction mechanisms [2]. Ultrafast lasers allow one to characterize temporally electron mediated processes [3–5] and also to measure the energy flow between electrons and adsorbate degrees of freedom [6–8]. However, a comprehensive and predictive understanding is still to be achieved. For example, the prototype CO or NO photodesorption is phonon mediated on certain metals such as Ru and electron mediated on others such as Cu, Pd, and Pt, in a, so far, nonpredictive way. Similarly, observed site selectivities [including the case of CO/Pt(111) [9]] are hard to rationalize. In this work, we use sum frequency generation (SFG) to probe CO coverage on Pt(111) in ultrafast pump-probe experiments. We show that SFG can be used to measure the photodesorption yield in a broad range of CO coverage using a steady state approach and varying the CO pressure and the pump laser fluence. We observe a dramatic effect of coverage on the photodesorption rate constant, which seems to be related to electron delocalization in the CO $2\pi^*$ states involved in photodesorption.

The Pt(111) sample is prepared under UHV using standard methods (Ar ion bombardment, annealing to 900 °C, heating under 10^{-7} mbar of O_2), and controlled using Auger electron spectroscopy and LEED. An amplified Ti:sapphire laser at 800 nm pumps at 1 kHz an optical parametric amplifier (OPA). The OPA produces tunable IR radiation between 1 and 10 μm. The residual beam at 800 nm is split into a pump beam (up to 50 μJ, 130 fs), and a probe beam, the linewidth and wavelength of which is adjusted by means of a pulse shaper. Vibrationally resolved SFG spectra are obtained by overlapping this ≈ 2 μJ, ≈ 4 ps, ≈ 4 cm^{-1} FWHM "visible" beam and the ≈ 3 μJ, ≈ 145 fs, ≈ 150 cm^{-1} FWHM IR beam onto the sample in a copropagating, colinear configuration. The spectral resolution in SFG depends only on the bandwidth of the visible laser and spectra can be acquired in the spectral range covered by the IR pulse without scanning the frequency [10,11]. The beams are spectrally filtered and dispersed by a monochromator on a 512 pixel CCD camera which allows one to record SFG spectra in a region of 310 cm^{-1} centered at ca. 700 nm. The measured spectrum is readily converted into a vibrational spectrum by subtracting the frequency of the visible probe beam. We have checked that sample heating due to the pump beam cannot bias our results [8].

Figure 1(a) shows a series of SFG spectra recorded at specified delays after a pump pulse at 800 nm. A full analysis of the pump-probe spectra is reported elsewhere [8]. It is based on a similar model as in [6,7]. A two temperature model [12] is used to evaluate the time resolved electron, phonon, and adsorbate vibrational mode temperatures (Fig. 2). SFG emission is calculated in the time domain using the inputs of the two temperature model and of anharmonic coupling of CO internal vibration with the lower frequency Pt-CO modes. Two modes must be invoked as for CO/Ru(0001) [7], but in contrast to this system a direct interaction between electrons and frustrated rotation with a time scale <200 fs is found for Pt(111).

In this Letter, we focus on the photodesorption yield. The CO band is not measurably different before (delay, -5 ps) and after (200 ps) the pump pulse, showing that the change in CO coverage θ_{CO} in a single pulse is smaller than our noise limit of $\approx 10^{-2}$ monolayer (ML) [1 ML $= 1.5 \times 10^{15}$ cm^{-2}, the density of atoms on Pt(111)]. This is not unexpected: a desorption yield smaller than 10^{-3} ML was reported for CO/Pt(111) at absorbed fluences <35 J m^{-2} [13]. However, photodesorption can be shown to occur from our data. We collect spectra at 1 kHz under steady state conditions of photodesorption and readsorption. Therefore, the CO coverage is limited by readsorption. The adsorption between two laser pulses has the form

$$(d\theta_{CO})_{ads} = s(\theta_{CO}) P_{CO} \delta t / L_1, \quad (1)$$

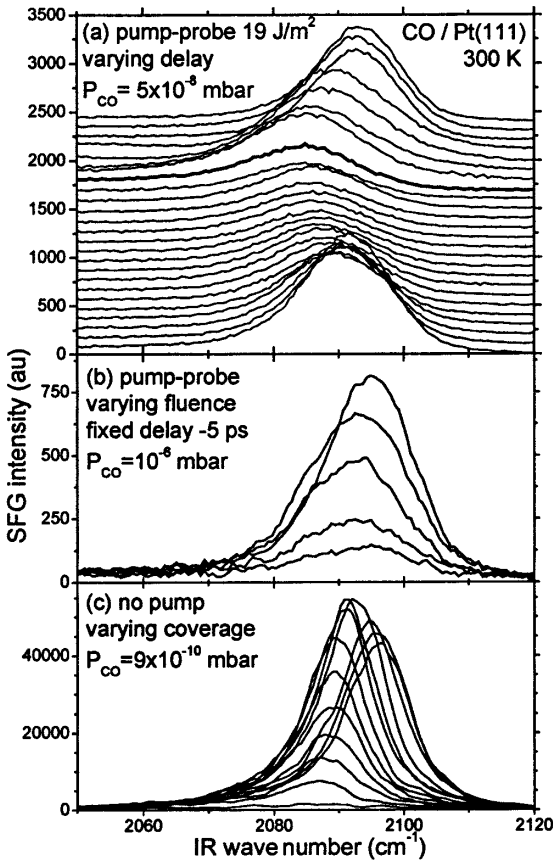

FIG. 1. SFG spectra of CO on Pt(111) at 300 K: (a) pump-probe spectra as a function of delay between pump and IR probe lasers; delays are −10, −5, −3, −1, −0.75, −0.5, −0.25, 0, 0.25, 0.5, 0.75, 1, 1.5, 2, 2.5, 3, 4, 5, 7.5, 10, 30, 40, 50, 75, and 100 ps from top to bottom. (b) Pump-probe spectra at a fixed delay (− 5 ps) as a function of pump laser fluence; fluences are 14, 27, 41, 55, and 70 J/m^2 from top to bottom, and the corresponding estimated coverages are 0.36, 0.26, 0.22, 0.14, and 0.10 ML. (c) Spectra as a function of CO coverage as collected during CO adsorption at low pressure; estimated coverages are 0.03, 0.08, 0.11, 0.15, 0.19, 0.22, 0.25, 0.28, 0.29, 0.32, 0.36, 0.38, and 0.44 ML. The peak frequency shifts to the blue continuously with coverage. The intensity of linear sites decreases above 0.33 ML because a fraction of molecules occupies bridge sites.

where $s(\theta_{CO})$ is the sticking coefficient (Fig. 3); $P_{CO}\delta t/L_1$ is the number of CO molecules (in ML) impinging onto a unit surface during one period ($\delta t = 1$ ms) of the laser. Expressing P_{CO} in mbar, $L_1 = \sigma(TM)^{0.5}/2.67 \times 10^{22}$ mbar s [15], with T the temperature in K, M the molar mass of CO in g, and $\sigma = 1$ ML $= 1.50 \times 10^{15}$ cm^{-2}. At the surface temperature of 300 K used in this work, $L_1/\delta t = 5 \times 10^{-3}$ mbar. It follows that at 5×10^{-8} mbar the desorption yield is 10^{-5} ML/pulse. We observe that the steady state coverage is smaller than the saturation coverage, but much larger than 10^{-5} ML. Therefore, the desorption yield is larger than 10^{-5} ML/pulse at saturation and decreases with coverage. To quantify this variation, we express the steady state conditions. The photodesorption induced by a single pulse of absorbed fluence F can be written in the standard form

$$(d\theta_{CO})_{des} = k(\theta_{CO})\theta_{CO}F^n. \quad (2)$$

With this definition, a dependence of $k(\theta_{CO})$ on coverage corresponds to a deviation from a first order desorption rate. The exponent n was found to range from 7.3 for a pulse duration 125–155 fs to 9.1 for 205–285 fs [13]. Under steady state conditions (1) and (2) result in

$$k(\theta_{CO}) = s(\theta_{CO})P_{CO}\delta t/(L_1\theta_{CO}F^n). \quad (3)$$

At a given coverage, obtained for two different combinations (P_1, F_1) and (P_2, F_2) of P_{CO} and F, n is given by

$$n = \ln(P_1/P_2)/\ln(F_1/F_2). \quad (4)$$

We have measured a series of SFG spectra at −5 ps delay with P_{CO} and F varying in the range 5×10^{-8} to 2.5×10^{-5} mbar, and 14 to 70 absorbed J/m^2, respectively [Fig. 1(b)]. We obtain $n = 7.3 \pm 1$, the average of three

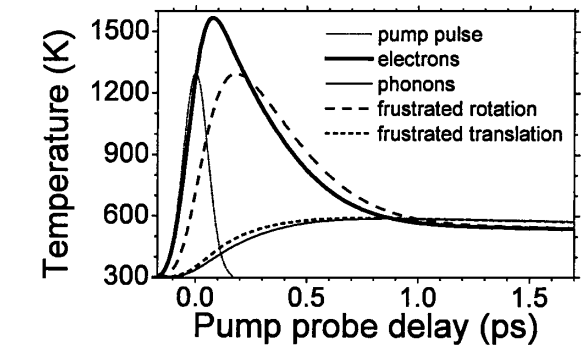

FIG. 2. The two temperature model applied to CO/Pt(111). The absorbed laser fluence is 19 J/m^2. Also shown are the temperatures of frustrated rotation and frustrated translation as extracted from full simulation of pump-probe spectra [8].

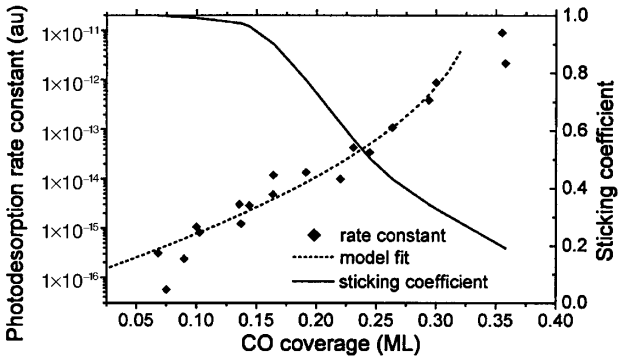

FIG. 3. Photodesorption rate constant as a function of CO coverage as derived from the kinetic steady state analysis of SFG spectra, and result of the model fit (see the text). The model is not appropriate for coverages above 0.33 ML. Also shown is the sticking coefficient as a function of coverage [14] used in the data analysis.

measurements at $\theta_{CO} = 0.22$, 0.15, and 0.10 ML, which indicate no trend of variation with coverage, and in agreement with Ref. [13], suggesting that our steady state approach is correct. In Ref. [13], n is derived from an entirely different type of data, namely, time of flight mass spectrometry.

We have recorded independently SFG spectra as a function of CO coverage in the absence of the pump laser [Fig. 1(c)] in order to extract the coverage from the pump-probe spectra. The variation of SFG intensity with coverage turns out to be quite similar to that of the Fourier-transform infrared absorbance, with a maximum at ≈ 0.33 ML where linear sites are most populated [16]. With n and the dependence of SFG intensity with θ_{CO}, we can calculate $k(\theta_{CO})$ using Eq. (3) for each pump/probe spectrum, taking $s(\theta_{CO})$ from the literature [14] (Fig. 3). The result is shown in Fig. 3. It reveals a decrease of the rate constant by ≈ 5 orders of magnitude from 0.37 to 0.07 ML.

Before we discuss this result, we come back to details of the pump-probe spectra. Comparison of Figs. 1(b) and 1(c) reveals that the CO bandwidth is larger for pump-probe spectra at -5 ps delay (where direct influence of the pump is excluded) than for spectra without the pump. A shoulder at $\approx 2085\ \mathrm{cm}^{-1}$ appears at 0.26 ML and below, and the CO band frequency does not decrease with coverage below 0.2 ML in the pump-probe spectra. This shows that the CO layer is partly disordered by the ultrafast laser excitation. It might be that at low coverage some CO occupy bridge sites, which are not probed in this work. In such a case, θ_{CO} would be underevaluated. According to (3), $k(\theta_{CO})$ would then be overevaluated, and since the disorder appears at low coverage, the variation of k with θ_{CO} would be even larger than in Fig. 3. In addition, photodesorption from bridge sites is at least 4 times less efficient than from linear sites [9], which reduces quantitatively the possible impact of bridge sites on our kinetic analysis. We can safely conclude that k does vary by at least 5 orders of magnitude.

The generally accepted photodesorption mechanism can be sketched as follows: (a) $Pt + h\nu \rightarrow Pt^*$; (b1) $Pt^* + CO_{ads} \rightarrow Pt + CO_{ads}{}^*$; (b2) $CO_{ads}{}^* \rightarrow CO_{ads}{}^{*\#}$; (c) $Pt + CO_{ads}{}^{*\#} \rightarrow Pt^* + CO_{ads}{}^{\#}$; (d) $CO_{ads}{}^{\#\#} \rightarrow CO_{gas}$; (e) $Pt^* \rightarrow Pt^{\#}$. Photons are absorbed by Pt at step (a). Pt^* refers to a distribution of excited electrons resulting from processes of time scales below 1 fs (absorption, electron diffusion, and electron-electron collisions). Electronic energy is transferred at steps (b1) and (b2) from electrons to CO degrees of freedom through a MGR-type mechanism [1]. Electrons are temporarily transferred into the CO $2\pi^*$ band. $CO_{ads}{}^*$ and $CO^{\#}$ correspond, respectively, to electronically and vibrationally excited CO. Step (c) is the return of excited electrons into bulk Pt. $CO_{ads}{}^{\#\#}$ designates the fraction of $CO^{\#}$ which have gained enough energy to desorb at step (d). Step (e) is the relaxation of Pt electronic excitation to phonons. Equilibrium between electrons and phonons is achieved in Pt in ≈ 1 ps (this value increasingly slightly with laser fluence) (Fig. 2).

We now discuss which steps of the desorption mechanism can be influenced by CO coverage. Steps (a) and (e) can hardly be affected by CO coverage. At step (b1) the CO coverage can influence the rate of energy transfer from Pt electrons to CO by modifying the work function, hence the energy of the CO $2\pi^*$ band relative to Fermi level. The band dispersion can also change due to increased CO-CO interactions (although the dispersion due to Pt-CO interaction is much larger). The probability P of electron attachment of $2\pi^*$ during a laser pulse can be evaluated in the form [4]

$$P = \iint f(E, t)\mathrm{DOS}^*(E)dEdt, \tag{5}$$

where $f(E, t)$ is the energy distribution of the laser excited electrons at time t, approximated by a Boltzmann distribution $g[T_e(t)]$, where $T_e(t)$ (Fig. 2) is calculated by the two temperature model [8]. We describe the $2\pi^*$ band by a normalized Gaussian distribution of width 0.3 eV centered at 2 eV above Fermi level at zero coverage, and 1.85 eV at 0.33 ML [14]. Two photon photoemission spectroscopy (2PPE) reveals no variation of the CO $2\pi^*$ bandwidth with coverage between 0.10 and 0.50 ML [17]. We have corrected the energy of CO states in 2PPE to account for the different nature of states involved in 2PPE and in photodesorption [18]. We find that P varies with coverage by a factor of ≈ 2 at 42 J/m^2 absorbed fluence.

At the desorption step (d), the desorption yield can depend on coverage through the decrease of desorption energy from 1.5 to 1.3 eV with increasing coverage between 0 and 0.33 ML [14]. Assuming that desorption proceeds thermally at this step with the temperature T_{ads} of frustrated rotation, the desorption probability increases by a factor ≈ 3 (at 42 absorbed J/m^2) at 0.33 ML with respect to zero coverage. Another effect of coverage can occur at step (d), namely, a dynamical effect related to CO-CO collisions which enhance at large coverage energy transfer into CO motion perpendicular to the surface. This effect is not demonstrated experimentally, but its calculated impact on the desorption yield dependence on coverage is 1.5 for CO/Cu(100) using molecular dynamics calculations [19]. This impact is expected to depend on the metal-CO potential energy surface and could perhaps be larger on Pt. If all desorption events were due to CO-CO collisions, a second order kinetics would result, with a desorption yield proportional to $\theta_{CO}{}^2$ (instead of θ_{CO}), leading to an increase of $k(\theta_{CO})$ by 5.3 from 0.07 to 0.37 ML. Therefore the expected impact of CO-CO collisions on the coverage dependence of the desorption rate is at most 5.3.

It results from the above estimates that work function and desorption energy together with dynamics of CO-CO collisions can account only for a desorption yield decrease

with decreasing coverage by about ≈ 1 order of magnitude instead of the experimental 5 orders of magnitude. Thus, a much more dramatic effect must be present. Let us consider the possibility that at step (c) the lifetime of excited electrons in the CO layer decreases with decreasing coverage. At 0.33 ML the CO layer is entirely ordered with the $(\sqrt{3}x\sqrt{3})R30°$ structure, and CO states have a well-defined parallel momentum $\mathbf{k}_{\parallel}$. When an electron is attached into the $2\pi^*$ band, it has a 2D motion according to its value of $\mathbf{k}_{\parallel}$. As coverage decreases below 0.33 ML, the CO layer keeps locally the same structure, but with defects consisting of missing CO. The defects imply an increasing tendency of excited $2\pi^*$ electrons to be diffused back into the bulk in a time $\tau_{\mathrm{exc}}(\theta_{\mathrm{CO}})$ decreasing with increasing defect density. Let us express $\tau_{\mathrm{exc}}(\theta_{\mathrm{CO}})$ as $\tau_{\mathrm{hop}} n(\theta_{\mathrm{CO}})$, where $n(\theta_{\mathrm{CO}})$ is the number of CO molecules "visited" by the electron before it is scattered back into the bulk and τ_{hop} is the inverse of the hopping frequency from a CO molecule to the next. In the multiple excitation extension of the MGR model [4], the desorption rate scales as $\exp[-\tau_{\mathrm{des}}/(\tau n)]$, with τ_{des} the time required for CO^* to evolve into the configuration of no return leading to desorption. τ_{des} is characteristic of the CO^* dynamics and does not change with coverage. It was estimated to be 12 fs by modeling the MGR process in the case of CO/Cu [4]. τ is the excitation lifetime of an individual molecule and $n = n_0$, the number of sequential excitations per molecule, as determined by the laser fluence. If we take into account electron delocalization within the CO layer, $\tau = \tau_{\mathrm{hop}}$, and $n = n_0 n(\theta_{\mathrm{CO}})$, because each electron attached to the CO layer now interacts sequentially with $n(\theta_{\mathrm{CO}})$ molecules. Therefore the desorption scales as $\exp[-\tau_{\mathrm{des}}/(\tau_{\mathrm{hop}} n_0 n(\theta_{\mathrm{CO}}))] = \exp[-\tau_{\mathrm{des}}/(\tau_{\mathrm{exc}}(\theta_{\mathrm{CO}}) n_0)]$, with $\tau_{\mathrm{exc}}(\theta_{\mathrm{CO}})$ the lifetime of electronic excitation in the whole layer. Assuming that electrons are diffused back to Pt at each collision with a defect, $\tau_{\mathrm{exc}}(\theta_{\mathrm{CO}})$ can be modeled as the ratio of the average distance between two missing CO to the velocity v of electron diffusion in the $2\pi^*$ band: $\tau_{\mathrm{exc}}(\theta_{\mathrm{CO}}) = a[\theta_{\mathrm{CO}}{}^{\mathrm{sat}}/(\theta_{\mathrm{CO}}{}^{\mathrm{sat}} - \theta_{\mathrm{CO}})]^{1/2}/v$, with $a = 4.81$ Å the nearest neighbor distance in the CO structure at $\theta_{\mathrm{CO}}{}^{\mathrm{sat}} = 0.33$ ML. We take $\tau_{\mathrm{des}}/n_0 = 12$ fs and fit the experimental data with v as a single parameter (Fig. 3). The experimental results are well reproduced with $v = 5.15$ Å/fs, corresponding to a CO-CO hopping time of 0.93 fs, and to a kinetic energy of 0.75 eV assuming a free electron. These values do not seem unrealistic. The CO $2\pi^*$ electrons diffuse from, and return to, the largely dispersed Pt $6p_x$ and $6p_y$ bands (where electrons are nearly free) which cross the CO $2\pi^*$ band. The Pt bulk states most coupled to CO $2\pi^*$ are those which correspond to the crossing, ≈ 2 eV above Fermi level: they presumably have several eV of kinetic energy. Above 0.33 ML, the surface defects are due to excess CO and correspond to the walls between $(\sqrt{3}x\sqrt{3})R30°$ and $c(4 \times 2)$ domains of local coverage 0.33 and 0.5 ML, respectively. We did not model this coverage range because we have only two experimental points above 0.33 ML, but these points do seem to obey a different model.

In conclusion, we measure a dramatic decrease of the photodesorption yield with decreasing coverage, which can be attributed to the decreased lifetime of electronic excitation in the CO layer. This emphasizes the importance of electron delocalization in the CO $2\pi^*$ states involved in photodesorption.

*Corresponding author.
Electronic address: bernard.bourguignon@ppm.u-psud.fr

[1] D. Menzel, Nucl. Instrum. Methods Phys. Res., Sect. B **101**, 1 (1995).
[2] M. Brandbyge, P. Hedegård, T. F. Heinz, J. A. Misevich, and D. M. Newns, Phys. Rev. B **52**, 6042 (1995).
[3] F. Budde, T. F. Heinz, M. M. T. Loy, J. A. Misewich, F. de Rougement, H. Zacharias, Phys. Rev. Lett. **66**, 3024 (1991).
[4] J. A. Prybyla, H. W. K. Tom, and G. D. Aumiller, Phys. Rev. Lett. **68**, 503 (1992).
[5] M. Bonn, S. Funk, C. Hess, D. N. Denzler, C. Stampfl, M. Scheffler, M. Wolf, and G. Ertl, Science **285**, 1042 (1999).
[6] T. A. Germer, J. C. Stephenson, E. J. Heilweil, and R. R. Cavanagh, J. Chem. Phys. **98**, 9986 (1993).
[7] M. Bonn, C. Hess, S. Funk, J. H. Miners, B. N. J. Persson, M. Wolf, and G. Ertl, Phys. Rev. Lett. **84**, 4653 (2000).
[8] F. Fournier, W. Zheng, S. Carrez, H. Dubost, and B. Bourguignon [J. Chem. Phys. (to be published)].
[9] K. Fukutani, M.-B. Song, and Y. Murata, J. Chem. Phys. **103**, 2221 (1995).
[10] E. W. M. van der Ham, Q. H. F. Vrehen, and E. R. Eliel, Opt. Lett. **21**, 1448 (1996).
[11] L. J. Richter, T. P. Petralli-Mallow, and J. C. Stephenson, Opt. Lett. **23**, 1594 (1998).
[12] S. I. Anisimov, B. L. Kapeliovich, and T. L. Perel'man, Zh. Eksp. Teor. Fiz. **66**, 776 (1974) [Sov. Phys. JETP **39**, 375 (1974)].
[13] L. Cai, X. Xiao, and M. M. T. Loy, Surf. Sci. **464**, L727 (2000).
[14] G. Ertl, M. Neumann, and K. M. Streit, Surf. Sci. **64**, 393 (1977).
[15] *Introduction to Surface Chemistry and Catalysis*, edited by G. A. Somorjai (John Wiley and Sons, New York, 1994), p. 13.
[16] B. E. Hayden and A. M. Bradshaw, Surf. Sci. **125**, 787 (1983).
[17] T. Anazawa, I. Kinoshita, and Y. Matsumoto, J. Electron Spectrosc. Relat. Phenom. **88–91**, 585 (1998).
[18] L. Cai, X. Xiao, and M. M. T. Loy, Surf. Sci. **492**, L688 (2001).
[19] C. Springer and M. Head-Gordon, Chem. Phys. **205**, 73 (1996).